23. M. Delmotte, thesis, Univ. Joseph Fourier, Grenoble, France (1997).
24. G. Delaygue, V. Masson, J. Jouzel, R. D. Koster, R. J. Healy, *Tellus* **52B**, 19 (2000).
25. M. Werner, M. Heimann, G. Hoffmann, *Tellus* **53B**, 53 (2001).
26. P. Ciais, J. Jouzel, *J. Geophys. Res.* **99**, 16793 (1994).
27. F. Bassinot *et al.*, *Earth Planet. Sci. Lett.* **126**, 91 (1994).
28. CLIMAP Project Members, *Map and Chart Series*, (Geological Society of America, Boulder, CO, Map Chart 36, 1981).
29. S. Joussaume, K. E. Taylor, *World Clim. Res. Program* Publ. **92**, 425 (1995).
30. The performed Monte Carlo simulations take into account the analytical uncertainties and the tolerance level between deuterium and deuterium excess (*21*). Several simulations were performed varying either the SST or the relative humidity (h) or both (assuming a realistic relation between them based on the saturation curve). In all cases where the SST was allowed to vary, the obtained SST versus site temperature profiles always showed a time lag of 800 ± 50 years between the ACR and the OCR. The simulation that varied only h required huge variations to explain the isotopic changes. The other simulation (varying both SST and h) showed very weak variations in h (less than 10%).
31. G. Hoffmann, personal communication.
32. The beginning of the OCR occurs about 0.9 ky before the Younger Dryas period, which can be recognized in the Dome C methane record at about 12.3 ky B.P. The uncertainty of this time lag is about 0.5 ky, taking the uncertainties of the gas-ice age difference and the time resolution of the methane record into account (*13*).
33. H. J. Exton, J. Latham, P. M. Park, M. H. Smith, R. R. Allan, in *Oceanic Whitecaps and Their Role in Air-Sea Exchange Processes*, E. C. Monahan, G. Mac Niocaill, Eds. (Reidel, Dordrecht, Netherlands, 1986), pp. 175–193.
34. R. Röthlisberger *et al.*, *J. Geophys. Res.* **105**, 20565 (2000).
35. E. Monnin *et al.*, *Science* **291**, 112 (2001).
36. J. C. Stager, P. A. Mayewski, *Science* **276**, 1834 (1997).
37. S. Johnsen *et al.*, *Nature* **359**, 311 (1992).
38. This work is a contribution to EPICA, a joint European Science Foundation/European Commission (EC) scientific program, funded by the EC and by national contributions from Belgium, Denmark, France, Germany, Italy, the Netherlands, Norway, Sweden, Switzerland, and the United Kingdom. This is EPICA publication no. 28. In France, EPICA is supported by the Institut Français de Recherches et Technologies Polaires. We thank F. Vimeux, M. Delmotte, U. von Grafenstein, C. Waelbroeck, and K. Rodgers for their comments; O. Cattani and S. Falourd for their careful measurements; and our many colleagues involved in drilling, science, and logistics at Dome C.

8 February 2001; accepted 2 August 2001

Glacial Surface Temperatures of the Southeast Atlantic Ocean

Julian P. Sachs,[1]* Robert F. Anderson,[2] Scott J. Lehman[3]

A detailed record of sea surface temperature from sediments of the Cape Basin in the subtropical South Atlantic indicates a previously undocumented progression of marine climate change between 41 and 18 thousand years before the present (ky B.P.), during the last glacial period. Whereas marine records typically indicate a long-term cooling into the Last Glacial Maximum (around 21 ky B.P.) consistent with gradually increasing global ice volume, the Cape Basin record documents an interval of substantial temperate ocean warming from 41 to 25 ky B.P. The pattern is similar to that expected in response to changes in insolation owing to variations in Earth's tilt.

The Southern Hemisphere oceans are thought to be an important component of the global climate system, possibly regulating glacial-to-interglacial changes in atmospheric CO_2 concentrations (*1*) and, on millennial time scales, north-south climate asynchrony (*2, 3*). We therefore sought to evaluate the temperature history of the Cape Basin, in the southeast Atlantic Ocean, which has yielded some of the most detailed ocean climate records from the Southern Hemisphere (*2, 4*). Brisk cyclonic currents scour sediment within the basin and deposit it on rapidly accumulating drifts in the southern part, at the base of the Agulhas Ridge (*5*). Sea surface temperatures (SSTs) were determined in core TN057-21-PC2 (41°08′S, 7°49′E; 4981 m water depth) from one such drift by the alkenone paleotemperature technique (*6*) using previously established protocols (*7*) and the temperature calibration of Prahl *et al.* (*8, 9*) (Fig. 1). The robustness of this technique has been demonstrated with hundreds of globally dispersed surficial sediment samples, many of which were from near our study area in the southeast Atlantic (*10*). Our results confirm the timing and approximate magnitude of SST changes during deglaciation and during oscillations of Marine Isotope Stage 3 (MIS 3) inferred previously from oxygen isotope variations in planktonic foraminifera (*2, 11*). However, we also document a previously unrecognized long-term trend in SST occurring 41 to 18 ky ago.

Holocene SSTs in TN057-21-PC2 (~19°C, Fig. 1) exceed the climatological mean annual temperature above the core site by 6°C (*12*) as a result of the winnowing and focusing of sediment from the northern part of the Cape Basin (*5*) where annual mean SSTs reach 21°C (*12*). To confirm that variations in the intensity of horizontal sediment transport did not cause the observed variations in down-core SST, we measured the activity of unsupported ^{230}Th in the sediment and used this quantity to derive sediment focusing factors (*13, 14*). Focusing factors, defined as the ratio by which the flux of horizontally transported material exceeds that of sinking material, were evaluated with respect to SST and alkenone flux (Fig. 2). No correlation exists between focusing factors and either alkenone-derived temperatures (r^2 = 0.15, Fig. 2A) or ^{230}Th-normalized alkenone fluxes (r^2 = 0.06, Fig. 2B). We thus conclude that horizontal advection of sediment did not produce the observed down-core variations in alkenone-derived SSTs. The magnitude of the focusing factors (~10 to 20) and the geographic extent of the drift deposit itself (*5*) indicate that sediments were derived from a large region, further precluding a strong influence on our record by local changes in SST or by frontal movements. Rather, alkenone unsaturation ratios in core TN057-21-PC2 provide a regional temperature signal for the Cape Basin. A precise time scale registered to the Greenland GISP2 (Greenland Ice Sheet Project 2) ice core was derived for the core (Fig. 3A) by Stoner *et al.* (*15*) by synchronizing magnetic intensity variations in the sediment to cosmogenic ^{10}Be and ^{36}Cl variations in the ice (*16*).

The total amplitude of SST in our record is 6.5°C, with minimum values of 12.5°C ~40 ky B.P. (Fig. 3A) and maximum values of ~19°C in the Holocene (Fig. 1). Temperatures were between 12.5° and 16°C in MIS 3 (>27 ky B.P.), and between 13.5° and 19°C during MIS 2 and the transition to MIS 1 (Fig. 3A). Millennial-scale temperature excursions during MIS 3 are 1° to 3°C. Deglacial warming commenced at 17.5 to 19 ky B.P. and continued until at least 11 ky B.P., with a brief plateau at ~14 to 13 ky B.P. (Fig. 3A). The glacial-Holocene temperature increase of 5.5°C (13.5° to 19°C) is comparable to recent faunal-based estimates in the temperate southeast Atlantic (*17, 18*). The pattern and timing of deglacial warming is similar to ice core paleotemperature records from Antarctica (*3*), but differs markedly from records of deglaciation in the North Atlantic where warming was interrupted by a return to cold glacial conditions during the Younger Dryas episode (~13 to 12 ky B.P.) (*19*). Observed SST changes are thus consistent with the pioneering work of Charles and co-workers (*2, 11*), who inferred local Cape Basin SST variations from high-resolution records of planktonic foraminiferal δ^{18}O values in TN057-21-PC2 and nearby core RC11-83.

An unexpected finding, however, is the warming trend at 41 to 25 ky B.P., during

[1]Department of Earth, Atmospheric and Planetary Sciences, Massachusetts Institute of Technology, 77 Massachusetts Avenue, Room E34-254, Cambridge, MA 02139, USA. [2]Lamont-Doherty Earth Observatory, Post Office Box 1000, Columbia University, Palisades, NY 10964, USA. [3]Institute of Arctic and Alpine Research, Campus Box 450, University of Colorado at Boulder, Boulder, CO 80309, USA.

*To whom correspondence should be addressed. E-mail: jsachs@mit.edu

which SSTs increased by 3.5°C (12.5° to 16°C) amid widespread global cooling (*20*), then decreased by 2.5°C from 25 to 19 ky B.P. (Fig. 3A). Few other marine records from the Southern Hemisphere resolve this climate history in any detail, although it is suggested by SST records from the midlatitude Indian Ocean (*21–24*) which indicate warming of 1° to 3°C after ~45 ky B.P., followed by cooling into the Last Glacial Maximum (*25*). This is in contrast to a long-term trend of increasing planktonic $\delta^{18}O$ in TN057-21-PC2 and nearby core RC11-83 (*2, 11*), which we attribute to the isotopic effect on the ocean of increasing ice volume.

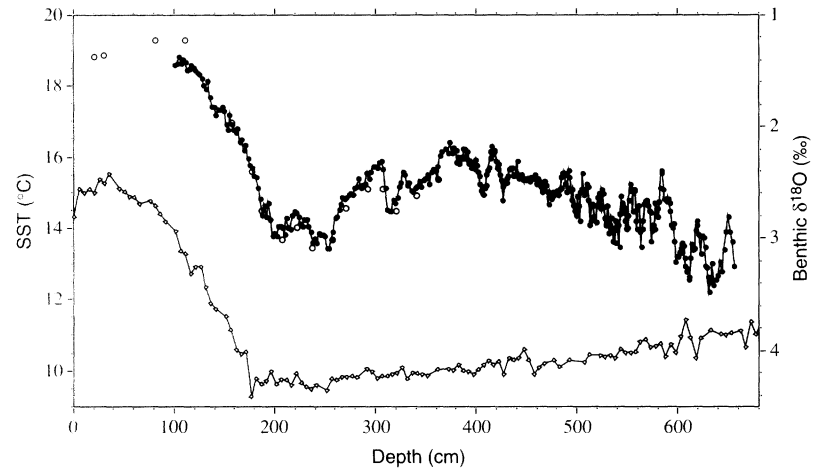

Fig. 1. SSTs derived from alkenone unsaturation ratios (*7, 9*) (circles; top trace) in core TN057-21-PC2. A benthic oxygen isotope stratigraphy (diamonds; bottom trace) was previously derived from the benthic foraminifera, *Cibicidoides* spp. (*4*). Open circles represent measurements performed on independently sampled sediment and, in the 100- to 380-cm interval, provide an indication of the reproducibility of the procedure. Alkenone analyses were performed on adjacent 1-cm samples from 380 to 630 cm, and on every other 1-cm interval from 100 to 380 cm and 630 to 656 cm, giving a temporal resolution of 60 and 120 years, respectively.

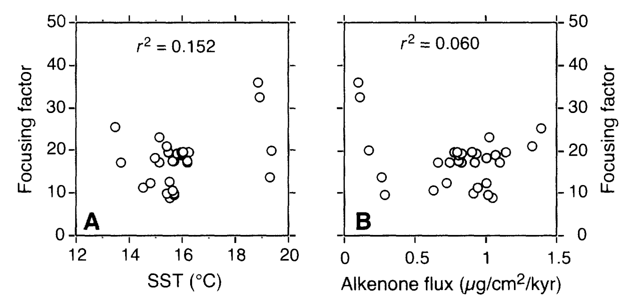

Fig. 2. Sediment focusing factors (*14*) are uncorrelated to both (**A**) alkenone-derived SST and (**B**) ^{230}Th-normalized alkenone fluxes, indicating that changing horizontal transport of fine-grained sediment did not cause the observed downcore variations in alkenone-derived temperatures.

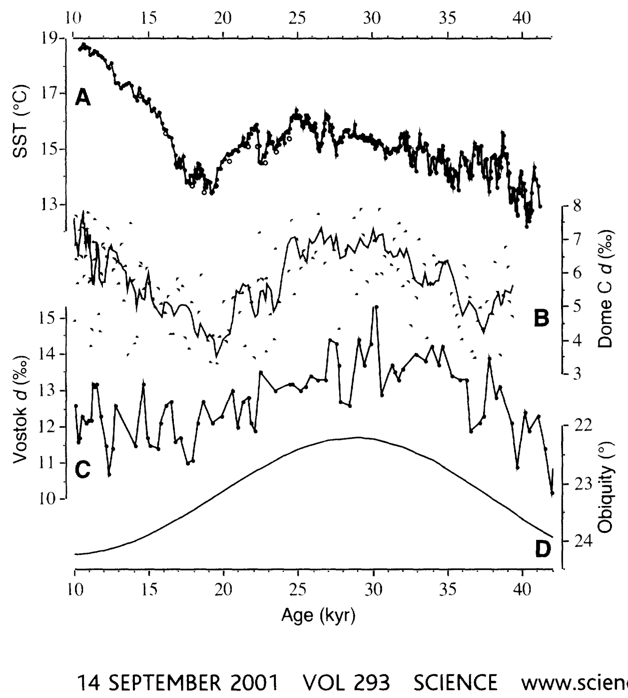

Fig. 3. (**A**) Cape Basin SSTs on the GISP2 time scale from Stoner *et al.* (*15*). (**B**) Deuterium excess, *d*, in the Dome C ice core (*26*). The solid line is a five-point running mean of the data. (**C**) Deuterium excess in the Vostok ice core (*27*) on the GRIP time scale (*3, 50*). (**D**) Obliquity variation through time with a reversed *y*-axis scale.

The SST progression bears a remarkable similarity to records of deuterium excess ($d = \delta D - 8 * \delta^{18}O$) in both Vostok and Dome C ice cores (East Antarctica) (*26, 27*) (Fig. 3, B and C). Deuterium excess is strongly influenced by kinetic isotope fractionation during evaporation, and both general circulation model and Rayleigh-type model simulations (*27–31*) indicate that a 1‰ change in central East Antarctic *d* reflects a 1° to 1.3°C change of temperature at the oceanic source (*29, 31*). Records of *d* in the Dome C (Fig. 3B) (*26*) and Vostok (Fig. 3C) (*27*) ice cores thus imply sea surface warming in the moisture-source regions of 2.5° to 3.5°C between ~40 and 27 ky B.P., and cooling of 2° to 3.5°C between ~27 and 18 ky B.P.

The observed correspondence between *d* and SST bears on the historical controversy surrounding the interpretation of deuterium excess. Although relative humidity, wind speed, and water vapor source temperature can all influence *d* (*26, 28, 32*), our results support recent studies indicating that *d* in central Antarctic snow is primarily a function of the water vapor source temperature (*31*). Corresponding changes in Cape Basin SST and central East Antarctic deuterium excess was at 41 to 18 ky B.P. imply either that (i) the southeast Atlantic was the primary moisture source for East Antarctica, (ii) a static East Antarctic moisture source region (or latitude band) underwent a similar temperature history as the Cape Basin, or (iii) the weighted-average temperature of East Antarctic moisture sources closely tracked changes in Cape Basin SST. Additional SST records are required to evaluate these possibilities. Model simulations indicating a subtropical and midlatitude Pacific and Indian Ocean source for contemporary central East Antarctic precipitation (*33, 34*) would appear to refute (i), and similar temperature changes implied by the alkenone and two deuterium excess records would not be expected in the case of (iii).

The temperature trends at 41 to 18 ky B.P. are inversely correlated with the obliquity component of insolation forcing (*35*) (Fig. 3D). The 41-ky obliquity cycle is also the predominant frequency in the 150,000-year record of precipitation-source temperatures inferred from deuterium excess in the Vostok ice core (*27*). Obliquity variations may modulate midlatitude temperatures in the Southern Hemisphere in part through direct solar forcing (*36*). Decreasing obliquity, such as that at 41 to 27 ky B.P. (Fig. 3D), produces opposing mean annual insolation changes at the top of the atmosphere at latitudes above and below ~45°S, with the low latitudes receiving more solar radiation and the high latitudes less (*37*). In response, climate models indicate that the low latitudes warm and the high latitudes cool (*36, 37*). The resultant increase of the meridional thermal gradient is reinforced by equatorward expansion of sea ice (*37*). Several feedbacks internal to the climate system may act on the altered temperature gradient to enhance warming in the Cape Basin and the temperate Southern Hemisphere oceans in general. These include reduced North Atlantic deep water (NADW) production (*36, 38*), enhanced Ekman heat transport from tropical to midlatitude surface waters (*39*), a poleward shift of the westerlies (*40*), and increased leakage of Agulhas Current water into the Atlantic (*41*).

Regardless of the mechanisms involved, an increasing meridional temperature gradient in the southeast Atlantic at ~41 to 25 ky B.P., inferred from increasing midlatitude SST relative to decreasing Antarctic air temperatures [δD and δ^{18}O of ice (*3*)], must have been associated with marked changes in transports of heat, moisture, and momentum. Furthermore, if the SST trends we document were more widespread, as the correspondence with deuterium excess suggests, they may have influenced climate globally via feedbacks involving water vapor and CO_2. Higher atmospheric water vapor and CO_2 concentrations are expected in response to warming of temperate Southern Hemisphere oceans at ~41 to 25 ky B.P., owing to the exponential dependence of water vapor pressure on temperature and diminished CO_2 solubility in warmer water, respectively.

Close covariation between southeast Atlantic SST and East Antarctic *d* provides an empirical link between those two parameters on orbital time scales and, if snow in central East Antarctica derived primarily from the subtropical and midlatitude Indian and Pacific Oceans, suggests that warming at ~41 to 25 ky B.P. was not confined to the Cape Basin. This warming must be reconciled with evidence for global ice growth derived from benthic oxygen isotope records (*42*). Sea ice and snow cover, which expand and persist longer into summer in response to decreased obliquity, may have facilitated high-latitude cooling via the ice-albedo feedback (*36, 37*), while direct solar forcing and feedbacks involving ocean circulation warmed the midlatitude Southern Hemisphere and increased the transport of moisture from the equator to the poles (*36*). Additional modeling studies of the Southern Hemisphere climate response to changing obliquity are needed to evaluate the relevant climate change mechanisms, whereas detailed SST records from other regions in the Southern Hemisphere are necessary to confirm the pattern and timing of glacial climate change there.

References and Notes

1. D. M. Sigman, E. A. Boyle, *Nature* **407**, 859 (2000).
2. C. D. Charles, J. Lynch-Stieglitz, U. S. Ninnemann, R. G. Fairbanks, *Earth Planet. Sci. Lett.* **142**, 19 (1996).
3. T. Blunier *et al.*, *Nature* **394**, 739 (1998).
4. U. S. Ninnemann, in *Mechanisms of Global Climate Change at Millennial Time Scales*, (*Geophys. Monogr.* **112**, American Geophysical Union, Washington, DC, 1999), pp. 99–112.
5. B. E. Tucholke, R. W. Embley, in *Interregional Unconformities and Hydrocarbon Accumulation*, J. S. Schlee, Ed. (American Association of Petroleum Geologists, Tulsa, OK, 1984), vol. 36, pp. 145–164.
6. S. C. Brassell, G. Eglinton, I. T. Marlowe, U. Pflaumann, M. Sarnthein, *Nature* **320**, 129 (1986).
7. J. P. Sachs, S. J. Lehman, *Science* **286**, 756 (1999).
8. F. G. Prahl, L. A. Muehlhausen, D. L. Zahnle, *Geochim. Cosmochim. Acta* **52**, 2303 (1988).
9. In this technique, the relative abundance of di- and triunsaturated C_{37} methyl ketones (alkenones) in the sediment is measured [$U^{k'}_{37} = C_{37:2}/(C_{37:2} + C_{37:3})$] and converted to SST using an empirically determined linear equation, $U^{k'}_{37} = 0.034{*}SST + 0.039$, derived from cultures of *Emiliania huxleyi* (*8*). Alkenones were extracted from 1 to 3 g of freeze-dried sediment using a pressurized fluid extractor (*7*). Alkenone concentrations ranged from 0.2 to 2 μg/g dry sediment. Precision of the procedure, based upon 28 analyses of our laboratory sediment standard (BRB) during the analysis of samples reported here, was 0.008 $U^{k'}_{37}$ units, or 0.2°C using the Prahl *et al.* (*8*) temperature calibration.
10. P. J. Müller, G. Kirst, G. Ruhland, I. V. Storch, A. Rosell-Mele, *Geochim. Cosmochim. Acta* **62**, 1757 (1998).
11. J. E. T. Channell, J. S. Stoner, D. A. Hodell, C. D. Charles, *Earth Planet. Sci. Lett.* **175**, 145 (2000).
12. S. Levitus, T. Boyer, *World Ocean Atlas 1994 Volume 4: Temperature* (U.S. Department of Commerce, Washington, DC, 1994), vol. NOAA Atlas NESDIS 4.
13. M. P. Bacon, *Chem. Geol.* **2**, 97 (1984).
14. The focusing factor is defined as the decay-corrected accumulation rate of unsupported ^{230}Th (disintegrations min^{-1} cm^{-2} ky^{-1}) divided by the production rate of ^{230}Th by U decay in the overlying water column (*13*). Unsupported ^{230}Th is the thorium that did not derive from uranium decay in the sediment.
15. J. S. Stoner, J. E. T. Channell, C. Hillaire-Marcel, C. Kissel, *Earth Planet. Sci. Lett.* **183**, 161 (2000).
16. The small adjustments (<1 ky from 41 to 10 ky B.P.) made to a previous chronology constructed by matching oxygen isotope variations to those in the well-dated nearby core RC11-83 (*4*) do not alter our conclusions. However, the Stoner *et al.* (*15*) time scale has the advantage of allowing direct comparison to GISP2 and paleoclimate records synchronized to it.
17. U. Brathauer, A. Abelmann, *Paleoceanography* **14**, 135 (1999)
18. A. Abelmann, U. Brathauer, R. Gersonde, R. Sieger, U. Zielinski, *Paleoceanography* **14**, 410 (1999).
19. S. J. Lehman, L. D. Keigwin, *Nature* **356**, 757 (1992).
20. Global cooling is indicated for this interval by increasing ice volume (*42*) and globally distributed marine (*43, 44*) and ice core (*3*) surface temperature proxies.
21. J. D. Hays, J. Imbrie, N. J. Shackleton, *Science* **194**, 1121 (1976).
22. J.-J. Pichon *et al.*, *Paleoceanography* **7**, 289 (1992).
23. L. Labeyrie *et al.*, *Paleoceanography* **11**, 57 (1996).
24. L. D. Labeyrie, J. C. Duplessy, *Palaeogeogr. Palaeoclimatol. Palaeoecol.* **50**, 217 (1985).
25. Additionally, an independent estimate of SST derived by subtracting benthic (*4*) from planktonic (*11*) foraminiferal δ^{18}O values in Cape Basin core TN057-21-PC2 yields a time series that corresponds in timing and magnitude with the alkenone results. This procedure attempts to remove the effect of global ice volume changes on ocean δ^{18}O values, leaving an isotopic record of temperature and salinity changes of the water in which the planktonic foraminifera lived. The magnitude and timing of the warming and cooling trends at 41 to 18 ky B.P. are similar in both records. This similarity ends during the latter part of the deglaciation when, given the large (~1.75‰) deglacial decrease in benthic δ^{18}O (Fig. 1), bottom water temperatures in the Cape Basin must have warmed substantially. Changes in surface salinity may also have affected planktonic δ^{18}O values.
26. J. Jouzel, L. Merlivat, C. Lorius, *Nature* **299**, 688 (1982).
27. F. Vimeux, V. Masson, J. Jouzel, M. Stievenard, J. R. Petit, *Nature* **398**, 410 (1999).
28. S. J. Johnsen, W. Dansgaard, J. W. C. White, *Tellus B* **41**, 452 (1989).
29. J. R. Petit, J. W. C. White, N. W. Young, J. Jouzel, Y. S. Korotkevich, *J. Geophys. Res.* **96**, 5113 (1991).
30. A. Armengaud, R. D. Koster, J. Jouzel, P. Ciais, *J. Geophys. Res.* **103**, 8947 (1998).
31. F. Vimeux *et al.*, *Clim. Dyn.* **17**, 503 (2001).
32. L. Merlivat, J. Jouzel, *J. Geophys. Res.* **84**, 5029 (1979).
33. R. D. Koster, J. Jouzel, R. J. Suozzo, G. L. Russell, *Clim. Dyn.* **7**, 195 (1992).
34. G. Delaygue, V. Masson, J. Jouzel, R. D. Koster, *Tellus B* **52**, 19 (2000).
35. The inverse correlation between SST and obliquity ends during the deglaciation, when ice sheets, greenhouse gas concentrations, and global thermohaline circulation change substantially. Forcings and feedbacks within the climate system must therefore overcome the obliquity forcing on Cape Basin temperatures. The corresponding increase of Cape Basin SST and Dome C *d* (Fig. 3, A and B) during the deglaciation, when Vostok *d* appears trendless (Fig. 3C), suggests that the moisture source for the two East Antarctic ice cores either diverged or experienced a different temperature history.
36. M. Khodri *et al.*, *Nature* **410**, 570 (2001).
37. R. G. Gallimore, J. E. Kutzbach, *J. Geophys. Res.* **100**, 1103 (1995).
38. Curtailment of NADW production warms the South Atlantic in particular, and the Southern Hemisphere in general, in many climate simulations as northward cross-equatorial heat transport is diminished and the surplus of heat is zonally advected throughout the Southern Hemisphere (*45*). Support for this mechanism comes from a time series of Cd/Ca in benthic foraminifera from the southwest Atlantic which is in-phase with obliquity (*46*) throughout the last 280 kyr, indicating diminished NADW production at low obliquity. In addition, δ^{13}C values in benthic foraminifera from core TN057-21-PC2, another proxy for thermohaline circulation, decreased between ~41 and 25 ky B.P. (*4*) as SSTs increased.
39. Westerly winds increase when the pole-equator temperature gradient increases in accord with the thermal wind relationship. Enhanced westerlies lead to stronger weather systems, enhanced eddy meridional momentum transport, and hence stronger surface winds. These enhanced surface winds impart momentum to the underlying ocean, leading to a proportional increase in Ekman heat transport from tropical to subtropical surface waters (*47*).
40. The meridional temperature gradient increases disproportionally poleward of 40°S (versus lower latitudes) in response to decreased obliquity (*37*). Because of the thermal wind relationship, the effect on surface westerlies and the latitude of zero wind-stress curl may therefore be a poleward shift, causing warm subtropical waters to also move poleward.
41. Presently, ~10% of Agulhas Current water leaks around South Africa transporting warm, salty subtropical Indian Ocean water to the South Atlantic, supplying 65% of surface and upper thermocline water (>9°C) to that basin (*48*). If low obliquity results in a poleward shift of the westerlies (*40*), the line of zero wind-stress curl would shift poleward and Agulhas leakage would increase (*49*). Because of extreme sensitivity to the separation between the line of zero curl and the African continent, simulated Agulhas leakage increases from near zero to near 100% with a 120-km (2°) poleward shift (*49*).
42. D. G. Martinson *et al.*, *Quat. Res.* **27**, 1 (1987).
43. M. R. Chapman, N. J. Shackleton, J.-C. Duplessy, *Palaeogeogr. Palaeoclimatol. Palaeoecol.* **157**, 1 (2000).
44. D. W. Lea, D. K. Pak, H. J. Spero, *Science* **289**, 1719 (2000).
45. S. Manabe, R. J. Stouffer, *J. Clim.* **1**, 841 (1988).
46. E. A. Boyle, in *Climate Processes and Climate Sensitivity*, J. E. Hansen, T. Takahashi, Eds. (American Geophysical Union, Washington, DC, 1984), Maurice Ewing vol. 5, pp. 360–368.
47. J. C. Marshall, A. J. G. Nurser, R. G. Williams, *J. Phys. Oceanogr.* **23**, 1315 (1993).
48. A. L. Gordon, R. F. Weiss, W. M. Smethie Jr., M. J. Warner, *J. Geophys. Res.* **97**, 7223 (1992).
49. W. P. M. de Ruijter, D. B. Boudra, *Deep-Sea Res.* **32**, 557 (1985).
50. A. Mazaud, F. Vimeux, J. Jouzel, *Earth Planet. Sci. Lett.* **177**, 219 (2000).

51. Discussions with J. Marshall improved this manuscript. Y. Chang, T. Keman, and M. Fleisher assisted in the laboratory. John Edmond provided laboratory space to J.P.S. This work is dedicated to his memory. The NSF provided support for this research.

19 June 2001; accepted 10 August 2001